η^6:η^6 Coordination of Tetraphenylborate to Ytterbium(II): A New Class of Lanthanoid *ansa*-Metallocenes

Glen B. Deacon,*[a] Craig M. Forsyth,[a] and Peter C. Junk[a]

Keywords: Metallocenes / Ytterbium / Tetraphenylborate / Bis(trimethylsilyl)amide / Pyrazolate

The ytterbium(II) complexes [Yb(*t*Bu$_2$pz)(THF)BPh$_4$] (**2**) (*t*Bu$_2$pzH = 3,5-di-*tert*-butylpyrazole) and [Yb{N(SiMe$_3$)$_2$}BPh$_4$] (**3**) were synthesised by reaction of [Yb{N(SiMe$_3$)$_2$}(THF)BPh$_4$] (**1**) with *t*Bu$_2$pzH or by in situ desolvation of the THF complex **1**. X-ray analysis of **2** and **3** reveals η^6:η^6 binding of chelating BPh$_4^-$ to ytterbium in both cases, generating true metallocene structures. Complex **3** is distinguished by a very short Yb–N bond and an agostic Yb–Me interaction, both indicative of a highly Lewis acidic metal centre.

Introduction

The recent rapid growth in the chemistry of lanthanoid-π-arene complexes has been fuelled both by an interest in their structures and bonding and by their ability to stabilise unusual oxidation states.[1–3] Readily available tetraphenylborate (BPh$_4^-$) can act as a chelating 12 e$^-$ donor through π bonding of two of the phenyl rings to a metal as in [Nb(RC≡CR)(η^6-Ph)$_2$BPh$_2$],[4,5] but not in lanthanoid tetraphenylborates, which almost exclusively have the BPh$_4^-$ simply in its classical counterion role (recent examples[6–13]). Two exceptions of note are [La(C$_5$Me$_5$){CH(SiMe$_3$)$_2$}BPh$_4$], for which the solid-state NMR spectra shows evidence of La–Ph interactions,[14] and structurally characterised [Sm(C$_5$Me$_5$)$_2$(Ph)$_2$BPh$_2$], which shows two of the Ph groups bound (η^2:η^2) to Sm^{3+}.[15] Both of these lanthanoid(III) complexes have two bulky coligands, which prevent a closer approach of BPh$_4^-$ to the metal centre. We have recently reported the isolation of the lanthanoid(II) tetraphenylborate, [Yb{N(SiMe$_3$)$_2$}(THF)(Ph)$_2$BPh$_2$] (**1**), which also has a bonded BPh$_4^-$ ligand.[16] However, the Yb–BPh$_4$ coordination is labile as indicated by the existence of two solid-state linkage isomers, one that has η^6-Ph:η^4-Ph binding to Yb (**1a**), whilst in the other isomer **1b**, an agostic Yb–Me(Si) bond and an η^1-Yb–Ph interaction replace the η^4-Ph donor.[16] Potentially, higher hapticity binding of the BPh$_4^-$ anion to Yb^{2+} may be induced by reducing either the steric bulk or the number of coligands. Following this design, we now report the synthesis and structures of two new ytterbium(II) tetraphenylborate complexes that show unequivocal η^6:η^6-Yb–Ph$_2$BPh$_2$ coordination.

[a] School of Chemistry, Monash University,
P. O. Box 23, Clayton, VIC, 3800, Australia
Fax: +61-3-9905-4597
E-mail: glen.deacon@sci.monash.edu.au

Results and Discussion

At low temperature, **1** reacts with one equivalent of *t*Bu$_2$pzH (3,5-di-*tert*-butylpyrazole) to give poorly soluble, red-purple [Yb(*t*Bu$_2$pz)(THF)BPh$_4$].2PhMe (**2**). A THF-free derivative of **1** was also prepared by in situ desolvation in PhMe to give purple [Yb{N(SiMe$_3$)$_2$}BPh$_4$] (**3**) (Scheme 1). Both compounds were obtained in moderate to good yields, and were characterised by analytical and spectroscopic data and by single-crystal X-ray structure determinations (see below). Solid-state IR spectra of **2** and **3** exhibit two ν(C=C$_{Ar}$) absorptions near 1580 cm^{-1} as well as three or more δ(C–H$_{Ar}$) bands between 700–800 cm^{-1}, consistent with the presence of both free and Yb-bound B–Ph moieties. However, in C$_6$D$_6$ solution at room temperature, only single Ph environments are observed in the ^{1}H NMR spectra of **2** and **3**. The *o*-H(Ph) resonances [δ: 8.14 (**2**), 7.84 (**3**) ppm] are shifted to higher frequency relative to free BPh$_4^-$, e.g. [Yb(MeCN)$_8$][BPh$_4$]$_2$ δ(CD$_3$CN) = 7.25 ppm[10] {compare also [Na([18]-cr-6)][BPh$_4$]·1.5H$_2$O δ(CD$_2$Cl$_2$) = 7.33 ppm[5]}, as has been observed for coordi-

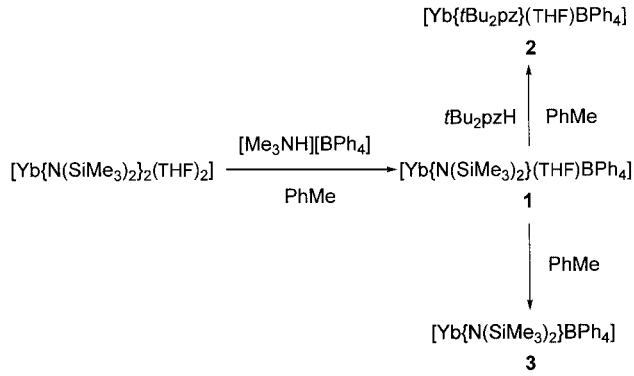

Scheme 1.

 DOI: 10.1002/ejic.200400953

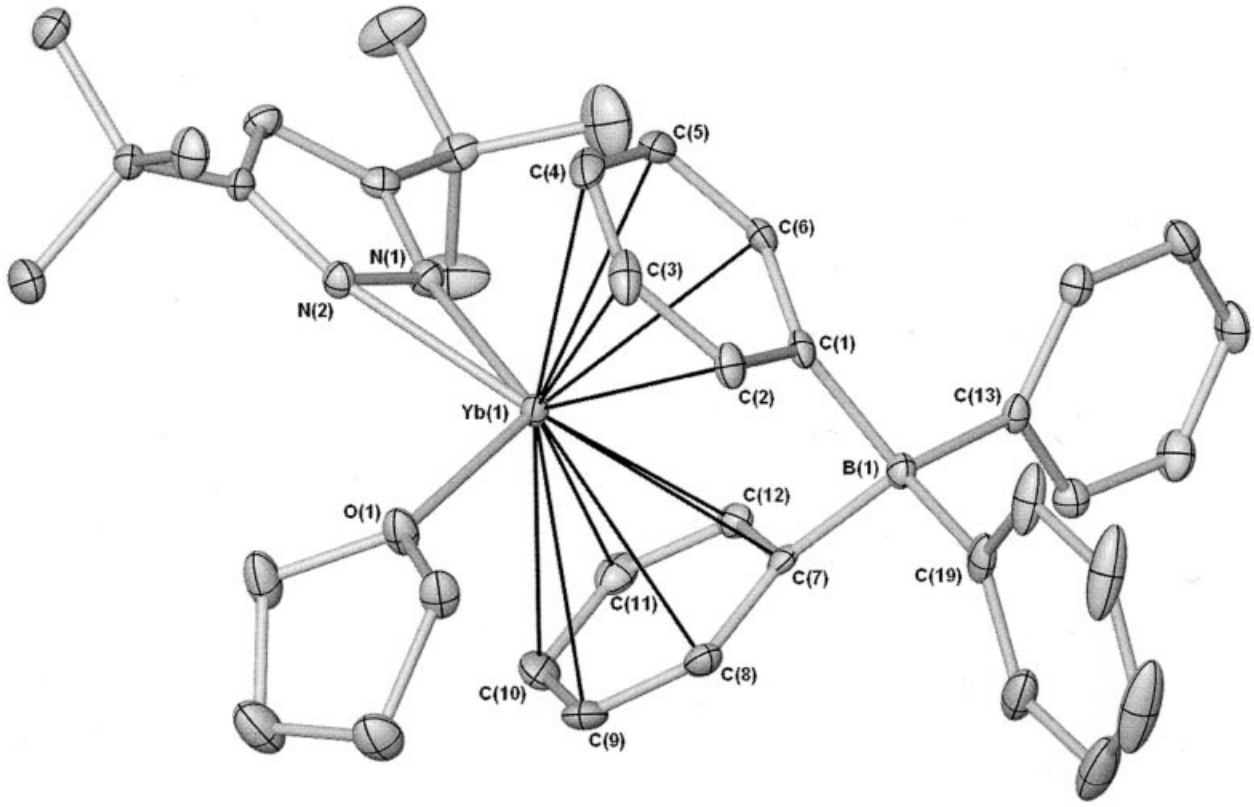

Figure 1. Molecular representation of the X-ray structure of [Yb(*t*Bu$_2$pz)(THF)BPh$_4$]·2C$_6$D$_6$ (**2a**) showing 50% thermal ellipsoids, and with lattice C$_6$D$_6$ molecules and hydrogen atoms omitted for clarity.

nation of BPh_4^- to other d^0 metals {e.g. [Zr(CH_2Ph)$_3$(η^6-Ph)BPh_3] δ_H = 8.25 ppm[17]}. Thus, the data for **2** and **3** suggest that some degree of Yb–Ph coordination occurs in C_6D_6 solution, rather than formation of ion pairs such as [Yb(L)(THF)$_n$(C_6D_6)$_2$][BPh_4] (L = *t*Bu$_2$pz, *n* = 1; L = N($SiMe_3$)$_2$, *n* = 0), but that the system is fluxional. Variable-temperature ^{13}C NMR studies of **3** in C_6D_6/PhMe (1:10) show some line broadening at –40 °C for the aromatic carbon atoms but this is insufficient to resolve the two Ph environments. Further cooling results in significant precipitation of solid **3**, and **2** was insoluble in this medium below room temperature. A ^{171}Yb or ^{29}Si NMR signal for **3** could not be located between –40 and +30 °C.

To clarify the exact bonding mode(s) for BPh_4^- in **2** and **3**, X-ray crystal structures of both complexes were determined. Difficulty was experienced in obtaining single crystals, since at room temperature or with heating, solutions of **2** or **3** slowly decompose, and deposit yellow, insoluble [Yb(BPh_4)$_2$].[18] However, suitable crystals of [Yb(*t*Bu$_2$pz)(THF)BPh_4]·2C$_6$D$_6$ (**2a**) were deposited from a warm C_6D_6 solution, along with the yellow solid, whilst **3** was crystallised by slow evaporation of a cold PhMe solution. The molecular diagrams are shown in Figure 1 and Figure 2, and selected bond distances and angles are listed in Table 1. A key feature of both structures is the unequivocal η^6-binding of *two* phenyl rings from a chelating BPh_4^- anion to each of the central ytterbium atoms. In addition, **2a** has an η^2-*t*Bu$_2$pz$^-$ anion and a coordinated THF molecule, giving a formal coordination number of nine. In contrast, the remaining coordination sphere of **3** is occupied solely by an *N*-bound N($SiMe_3$)$_2^-$ ligand supported for coordination saturation by a short Yb–Me interaction to one of the $SiMe_3$ groups. Thus, the coordination number is eight. Both complexes exhibit distorted pseudotetrahedral coordination geometries, as defined by the centroids of the bound Ph groups, and the THF oxygen atom, and the centre of the N–N bond for **2a** and the amido nitrogen atom and bound $SiMe_3$ carbon atom for **3**.

The Yb–C distance ranges for each interacting Ph ring in **2a** and **3** are narrow (0.12–0.19 Å), and the average Yb–C distances (Table 1) are comparable to those (2.85–2.99 Å) of the single η^6-Ph–Yb moieties of **1a** or **1b**,[16] despite the higher coordination number in the current complexes. The average Yb–C distances in **3** are shorter than those to a substituted neutral arene, e.g. <Yb–C> 2.94 Å in [(Yb(η^6-$C_6Me_3H_3$)($AlCl_4$)$_2$]$_n$·*n*(C_6H_6)[19] or <Yb–C> 2.96, 2.98 Å in [Yb{SC_6H_3-2-(η^6-$C_6H_2Pr^i_3$)-6-($C_6H_2Pr^i_3$)}$_2$].[20] With allowance for differences in coordination number, the upper limit for Yb–C bonding in **2a** and **3** [3.050(2) Å] is comparable with or well below the upper value for the preceding two complexes,[19,20] whilst the current Yb–C distance range (Table 1) is comparable or smaller. In the metallocene complex [Yb{N($SiMe_3$)$_2$}(C_5Me_5)$_2$Na(THF)$_3$],[21] which has an analogous ytterbium coordination environment to that of

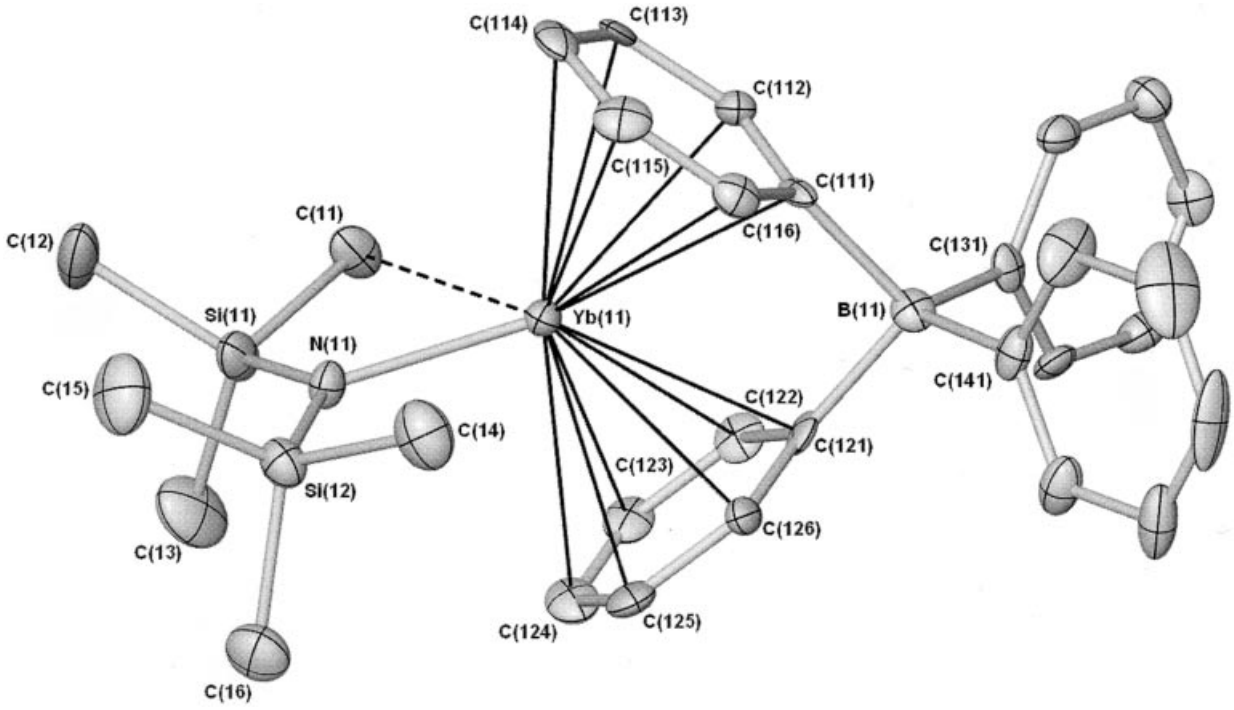

Figure 2. Molecular representation of the X-ray structure of [Yb{N(SiMe$_3$)$_2$}BPh$_4$] (**3**) showing 50% thermal ellipsoids, and with hydrogen atoms omitted for clarity. The agostic Yb–Me interaction is represented by a dotted bond. Only one of the virtually identical but crystallographically independent molecules is shown.

Table 1. Selected bond distances [Å] and angles [°] for **2a** and **3**. Entries Yb–C(Ph) refer to ranges for individual Ph rings with the average value in italics; Ph* refers to the centroid of a bonded η^6-Ph ring, N* refers to the centre of the N–N bond of the η^2-*t*Bu$_2$pz in **2a**. Complex **3** has two virtually identical independent molecules in the asymmetric unit, only values for one are listed.

	2a	**3**
Yb–C(Ph)	2.799(2)–2.945(2), *2.88* 2.860(2)–3.050(2), *2.95*	2.784(11)–2.899(11), *2.85* 2.810(7)–2.956(12), *2.87*
Yb–C(Me)		2.845(8)
Yb–N	2.351(2), 2.364(2)	2.262(6)
Yb–O	2.360(2)	
Si–C		1.854(9)–1.874(10), 1.915(8)[a]
Ph*–Yb–Ph*	112.8	114.0
Ph*–Yb–N/N*	123.5, 108.4	131.8, 110.8
Ph*–Yb–O/C	107.4, 104.4	111.5, 109.4
N/N*–Yb–O/C	98.4	67.9

[a] Si–C distance for the Me group bound to Yb.

3, the average Yb–C(C$_5$Me$_5$) bond length (2.83 Å) of the bridging (η^5:η^5) C$_5$Me$_5$ ligand is close to the average Yb–C distance in **3** (Table 1).

The amido ligands in both **2a** and **3** are characterised by short Yb–N distances, emphasising the high Lewis acidity of Yb^{2+} in the Yb(Ph)$_2$BPh$_2$ fragment. The two Yb–N distances in **2a** (Table 1) are approximately equivalent, indicating symmetrical binding of the *t*Bu$_2$pz$^-$ ligand, but the values are shorter than those of eight coordinate [Yb(Ph$_2$pz)$_2$(DME)$_2$] [2.414(7)–2.430(7) Å].[22] Similarly, the Yb–N distance in **3** [2.262(6) Å] is remarkably short relative to 2.41(2) Å in the closely related compound [Yb{N(SiMe$_3$)$_2$}(C$_5$Me$_5$)$_2$Na(THF)$_3$].[21] This difference is also likely to be influenced by the decreased steric bulk of **3** (two Ph groups compared with two C$_5$Me$_5$ groups) and the boron linkage in the chelating BPh$_4^-$ ligand, and this results in a more open residual coordination sphere. The centroid–Yb–centroid angle (Ph*–Yb–Ph* 114.0°) is significantly smaller for **3** than for [Yb{N(SiMe$_3$)$_2$}(C$_5$Me$_5$)$_2$Na(THF)$_3$] (Cp*–Yb–Cp* 134°).[21] The Ph*–Yb–Ph* angles are also considerably more acute than for BPh$_4^-$ in [Nb(RC≡CR)(η^6-Ph)$_2$BPh$_2$] (131.6°).[4] Complex **3** has a Yb–C(Me) distance [2.845(8) Å] that is much shorter than a similar interaction in **1b** [3.123(4) Å[16]) but comparable to those of [Yb{N(SiMe$_3$)$_2$}$_2$]$_2$ [2.785(4)–2.823(4) Å], which has several agostic Yb–Me$_3$Si interactions to support the YbN$_3$ coordination.[23] The Yb–Me contact is accompanied by a narrowing of the Yb–N–Si angle from 111.0(1)° in **1a** to 104.6(3)° in **3** and an apparent lengthening of the associated Si–C distance (Table 1).

Conclusions

Through the use of steric engineering that provides an appropriate coligand environment in heteroleptic Yb(L)BPh$_4$ complexes, stronger binding of BPh$_4^-$ to Yb^{2+} has been achieved with the first observation of η^6:η^6-Ph$_2$BPh$_2$ coordination to a lanthanoid. These complexes represent true *ansa*-metallocenes of ytterbium(II) and, in particular, the solvent-free complex **3** parallels the highly catalytically active *ansa*-bis(cyclopentadienyl)lanthanoid(III) species, and we are currently pursuing this aspect.

Experimental Section

General Remarks: All reactions were carried out under dry nitrogen or argon by using dry box and standard Schlenk techniques. Solvents were dried by distillation from sodium wire/benzophenone. Elemental analyses (C,H,N) were performed by the Campbell Microanalytical Service, University of Otago, New Zealand. IR data (4000–650 cm^{-1}) were recorded for Nujol mulls sandwiched between NaCl plates with a Perkin–Elmer 1600 Fourier transform infrared spectrometer. NMR spectra were obtained with a Bruker AC300 MHz spectrometer; [D_6]benzene was degassed and distilled from Na/K alloy prior to use. **1**,[16] [Yb{N($SiMe_3$)$_2$}$_2$(THF)$_2$],[24] Me_3NHBPh_4,[25] and 3,5-tBu$_2$pzH[26] were prepared according to literature procedures.

[Yb(tBu$_2$pz)(THF)BPh$_4$].2PhMe (2): A Schlenk flask was charged with tBu$_2$pzH (0.05 g, 0.25 mmol), **1** (0.18 g, 0.25 mmol), and PhMe (20 mL), and cooled to –40 °C. The reaction mixture was stirred and allowed to warm to 0 °C over approximately 1 h. The resulting purple solution was concentrated to 10 mL and cooled to –73 °C to yield **2** as a red-purple solid, which was collected and dried under vacuum (yield 0.14 g, 67%). IR (Nujol): $\tilde{\nu}$ = 1584 (w), 1570 (w), 1496 (m), 1310 (w), 1272 (w), 1248 (m), 1220 (w), 1184 (m), 1156 (m), 1066 (w), 1030 (m), 1014 (m), 993 (w), 934 (s), 869 (m), 857 (m), 777 (m), 750 (vs), 729 (vs), 714 (vs), 695 (m) cm^{-1}. ^{1}H NMR ([D_6]benzene): δ = 8.14 [br. s, 8 H, *o*-H(BPh)], 7.22 [br. s, 8 H, *m*-H(BPh)], 7.16–7.00 (m, 10 H, *Ph*Me), 6.90 [br. t, J = 7.5 Hz, 4 H, *p*-*H*(BPh)], 6.11 [br. s, 1 H, *H*4(pz)], 2.11 (s, 6 H, Ph*Me*), 1.24 (br. s, 18 H, tBu) ppm. Resonances due to THF at $\delta \approx$ 3.5 and 1.3 ppm (underlying the tBu resonance at δ = 1.24 ppm) were extremely broad with unreliable integration. Analytical data were consistent with loss of lattice toluene molecules: [Yb(t-Bu$_2$pz)(THF)BPh$_4$], $C_{39}H_{47}BN_2OYb$ (744.32): calcd. C 62.9, H 6.4, N 3.8%; found C 62.8, H 6.7, N 3.6% {compare with [Yb(t-Bu$_2$pz)(THF)BPh$_4$]·2PhMe, $C_{53}H_{63}BN_2Yb$ (928.44): calcd. C 68.5, H 6.8, N 3.0%}. Single crystals of [Yb(tBu$_2$pz)(THF)BPh$_4$]·2C_6D_6 (**2a**) were grown from a [D_6]benzene solution of **2**.

[Yb{N(SiMe$_3$)$_2$}BPh$_4$] (3): A Schlenk flask was charged with [Yb{N($SiMe_3$)$_2$}$_2$(THF)$_2$] (0.64 g, 1.0 mmol), Me_3NHBPh_4 (0.38 g, 1.0 mmol), and PhMe (60 mL), and the reaction mixture was stirred for 2 h at –10 °C. The solvent was then removed under vacuum whilst maintaining the solution at –10 °C. PhMe (60 mL) was added to the residue, and the mixture was stirred for a further 1 h at –10 °C before the solvent was again removed, and the cycle was repeated. After the final removal of solvent, PhMe (60 mL) was added, and the resulting purple solution was filtered, concentrated to 5 mL, and hexanes (10 mL) were added. Cooling to –73 °C gave **3** as a purple solid, which was collected and dried under vacuum (yield 0.36 g, 55%). IR (Nujol): $\tilde{\nu}$ = 1583 (w), 1560 (w), 1307 (w), 1249 (m), 1240 (m), 1178 (w), 1156 (m), 1066 (vs), 976 (w), 833 (m), 816 (m), 783 (w), 748 (s), 736 (s), 712 (s) cm^{-1}. ^{1}H NMR (300 MHz, 303 K, [D_6]benzene): δ = 7.84 [br. d, J = 5.8 Hz, 8 H, *o*-*H*(BPh)], 7.06 [br. s, 8 H, *m*-*H*(BPh)], 6.90 [br. s, 4 H, *p*-*H*(BPh)], –0.19 (s, 18 H, SiMe_3) ppm. ^{13}C NMR (75.5 MHz, [D_6] benzene): δ = 135.0 [*o*-*C*H(BPh)], 129.3 [*m*-*C*H(BPh)], 124.6 [*p*-*C*H(BPh)], 4.5 (SiMe_3) ppm. The resonance for the *ipso*-C (bound to B) was not detected. ^{11}B NMR (128.4 MHz, [D_6]benzene): δ = –3.85 ppm. $C_{30}H_{38}BNSi_2Yb$ (652.65): calcd. C 55.2, H 5.9, N 2.1; found C 54.9, H 5.9, N 2.1%.

X-ray Crystallographic Study: Crystals were mounted in an inert atmosphere under viscous oil onto a glass fibre. Low-temperature (123 K) data were collected on an Enraf–Nonius KAPPA CCD area-detector diffractometer (Mo-K_α radiation, λ 0.71073 Å, frames comprised 1.0° or 0.5° increments in φ and ω yielding a sphere of data) with proprietary software (Nonius B.V., 1998). Each data set was corrected for absorption (empirical-SORTAV[27]) then merged (R_{int} as quoted) to N unique reflections. The structures were solved by conventional methods and refined with anisotropic thermal parameter forms for the non-hydrogen atoms by full-matrix least-squares on all F^2 data by using SHELX 97.[28] Hydrogen atoms were included in calculated positions and allowed to ride on the parent carbon atom.

2a: $C_{51}H_{47}D_{12}B_1N_2O_1Yb_1$ (911.92) monoclinic $P2_1/n$, a = 15.0562(1), b = 16.2227(1), c = 18.1395(3) Å, β = 97.296(1) °, V = 4394.7(1) Å^3, $D_{calcd.}$ (Z = 4) 1.378 g cm^{-3}, μ_{Mo} = 2.166 mm^{-1}, F(000) 1848, $T_{min,max}$ = 0.561, 0.653, N_{total} = 50926, N = 10752 (R_{int} = 0.053), R = 0.026, wR_2 = 0.061 (R = 0.038, wR_2 = 0.064 all data). One of the lattice C_6D_6 molecules was disordered over two positions, and the geometries of both components were modelled as rigid hexagons.

3: $C_{30}H_{38}B_1N_1Si_2Yb_1$ (652.64) orthorhombic $Pca2_1$, a = 31.2276(4), b = 9.5779(1), c = 19.6904(3) Å, V = 5889(2) Å^3, $D_{calcd.}$ (Z = 8) 1.472 g cm^{-3}, μ_{Mo} = 3.28 mm^{-1}, F(000) 2624, $T_{min,max}$ 0.549, 0.778, x_{abs} 0.066 (12), N_{total} = 59936, N = 13425 (R_{int} = 0.096), R = 0.047, wR_2 = 0.082 (R = 0.086, wR_2 = 0.094 all data). As modelled in $Pca2_1$, the asymmetric unit comprised a pair of molecules apparently related by a centre of symmetry. However, no further crystallographic symmetry was detected by using the program PLATON,[29] and no sensible solution could be found in the centrosymmetric space group *Pbcm*. The high correlation matrix elements present in the noncentrosymmetric solution as a result of the pseudosymmetry presumably contribute to the relatively large ESDs.

CCDC-255023 and CCDC-255024 contain the supplementary crystallographic data for this paper. These data can be obtained free of charge from The Cambridge Crystallographic Data Centre via www.ccdc.cam.ac.uk/data_request/cif.

Acknowledgments

We thank the Australian Research Council for support.

[1] M. N. Bochkarev, *Chem. Rev.* **2002**, *102*, 2089–2117.
[2] G. B. Deacon, Q. Shen, *J. Organomet. Chem.* **1996**, *511*, 1–17.
[3] F. G. N. Cloke, *Chem. Soc. Rev.* **1993**, *22*, 17–24.
[4] F. Calderazzo, G. Pampaloni, L. Rocchi, U. Englert, *Organometallics* **1994**, *13*, 2592–2601.
[5] M. Aresta, E. Quaranta, I. Tommasi, *New. J. Chem.* **1997**, *21*, 595–613.
[6] S. Bambirra, M. W. Bouwkamp, A. Meetsma, B. Hessen, *J. Am. Chem. Soc.* **2004**, *126*, 9182–9183.
[7] G. B. Deacon, C. M. Forsyth, *Chem. Eur. J.* **2004**, *10*, 1798–1804.
[8] S. Arndt, T. P. Spaniol, J. Okuda, *Angew. Chem. Int. Ed.* **2003**, *42*, 5075–5079; *Angew. Chem.* **2003**, *115*, 5229–5233.
[9] W. J. Evans, J. M. Perotti, J. C. Brady, J. W. Ziller, *J. Am. Chem. Soc.* **2003**, *125*, 5204–5212.
[10] W. J. Evans, M. A. Johnston, M. A. Greci, T. S. Gummersheimer, J. W. Ziller, *Polyhedron* **2003**, *22*, 119–126.
[11] S. M. Cendrowski-Guillaume, G. Le Gland, M. Lance, M. Nierlich, M. Ephritikhine, *Compt. Rend. Chim.* **2002**, *5*, 73–80.
[12] R. Taube, S. Maiwald, J. Sieler, *J. Organomet. Chem.* **2001**, *621*, 327–336.
[13] G. A. Molander, R. M. Rzasa, *J. Org. Chem.* **2000**, *65*, 1215–1217.
[14] C. J. Schaverien, *Organometallics* **1992**, *11*, 3476–3478.
[15] W. J. Evans, C. A. Siebel, J. W. Ziller, *J. Am. Chem. Soc.* **1998**, *120*, 6745–6752.

[16] G. B. Deacon, C. M. Forsyth, *Chem. Commun.* **2002**, 2522–2523.
[17] M. Bochmann, G. Karger, A. J. Jager, *J. Chem. Soc. Chem. Commun.* **1990**, 1038–1039.
[18] [$Yb(BPh_4)_2$] was identified by IR spectroscopy and conversion to $[Yb(MeCN)_8][BPh_4]_2$.[10]
[19] S. I. Troyanov, *Russ. J. Coord. Chem.* **1998**, *24*, 351–358.
[20] M. Niemeyer, *Eur. J. Inorg. Chem.* **2001**, 1969–1981.
[21] Z. Hou, Y. Zhang, H. Tezuka, P. Xie, O. Tardif, T. Koizumi, H. Yamazkai, Y. Wakatsuki, *J. Am. Chem. Soc.* **2000**, *122*, 10533–10543.
[22] G. B. Deacon, E. E. Delbridge, B. W. Skelton, A. H. White, *Eur. J. Inorg. Chem.* **1999**, 751–761.
[23] R. Anwander, *Top. Curr. Chem.* **1996**, *179*, 32–112.
[24] G. B. Deacon, C. M. Forsyth, G. D. Fallon, H. Schumann, R. Weimann, *Chem. Ber./Recueil* **1997**, *130*, 409–415.
[25] P. K. Bakshi, A. Linden, B. R. Vincent, S. P. Roe, D. Adhikesavalu, T. S. Cameron, O. Knop, *Can. J. Chem.* **1994**, *72*, 1273–1293.
[26] J. Elguero, E. Gonzalez, J. Jacquier, *Bull. Soc. Chim. Fr.* **1968**, 707–713.
[27] R. H. Blessing, *Acta Crystallogr. Sect. A* **1995**, *51*, 33–37.
[28] G. M. Sheldrick, *SHELXL-97*, Universität Göttingen, **1997**.
[29] A. L. Spek, *PLATON*, Utrecht University, **2004**.

Received November 15, 2004

